

Near infrared and ultraviolet spectra of TLEs

F. J. Gordillo-Vázquez¹, A. Luque¹, M. Simek²

¹IAA - CSIC, Glorieta de la Astronomía s/n, 18008 Granada, Spain

²Department of Pulse Plasma Systems, Institute of Plasma Physics v.v.i., Academy of Sciences of the Czech Republic, Za Slovankou 3, 182 00 Prague, Czech Republic

Near infrared (NIR) and ultraviolet (UV) spectra of sprites, halos and beads corresponding to the first (1PG) and second positive (2PG) bands of N_2 have been calculated for different observation altitudes from mountains (3.25 km) to airplanes (14 km), balloons (35 km) and space (nadir) platforms. The calculated non-equilibrium vibrational distribution functions (VDF) of the $N_2(B^3\Pi_g)$ states in halos and beads show that the calculated NIR emissions produced through strong N_2 -1PG ($B^3\Pi_g \rightarrow A^3\Sigma_u^+$) transitions differ from the calculated sprite spectral emission patterns at ~ 888 nm but, particularly pronounced differences are found in the NIR spectral region at ~ 1046 nm and ~ 1231 nm corresponding to the N_2 -1PG (0,0) and (0,1) transitions, respectively. The blue near UV spectra from N_2 -2PG ($C^3\Pi_u \rightarrow B^3\Pi_g$) transitions in halos and beads also exhibits slightly different spectral features when compared to the blue – near UV spectrum of sprites for bands originating from higher v -levels ($v > 0$) although they might not be above noise level to be distinguished.

1. Objectives

Following the approach described in [1]-[2] we have calculated synthetic emission spectra of sprite streamers, halos and beads associated to their NUV and NIR optical emissions. To model the emission of the 1PG and 2PG systems of the neutral N_2 , we applied an approach based on calculating all allowed transitions between rotational manifolds of the upper and lower vibronic states arranged in a sequence of bands [3]-[4]. Here we considered all allowed rotational transitions between $N_2(C^3\Pi_u; v = 0 - 4)$ and $N_2(B^3\Pi_g; v = 0 - 12)$, and between $N_2(B^3\Pi_g; v = 0 - 12)$ and $N_2(A^3\Sigma_u^+; v = 0 - 20)$. After creating band profiles for all bands of a given system, we composed the complete spectrum of the 1PG and 2PG systems for the VDFs obtained by the kinetic modeling using the Einstein coefficients given in [5]. All bands were modeled assuming a Boltzmann rotational temperature of $T_R = 220$ K convolved with triangular line-shapes corresponding to resolutions of $\Delta\lambda = 3$ nm and $\Delta\lambda = 3.5$ nm for the 1PG and 2PG systems of N_2 , respectively. The NUV and NIR synthetic spectra for sprite streamers, halos and beads were calculated for observers located on mountains (3.25 km), aircrafts (14 km), balloon (35 km) and space platforms looking in the nadir.

2. Results

As can be seen in Figure 1, sprite, halo and sprite bead 1PG N_2 VDFs are quite similar from $v = 2$ through $v = 6$, which explains the similarity detected between sprite and halo spectral features in the visible (640 nm - 840 nm) region of the 1PG N_2 band emissions [1], [6]-[7]. No sprite bead spectral observations are published to date though, according to Figure 1a, bead optical emissions corresponding

to the $N_2(B^3\Pi_g)$ 1PG visible spectral range should exhibit quite similar (or the same) spectroscopic features to those of sprites and halos.

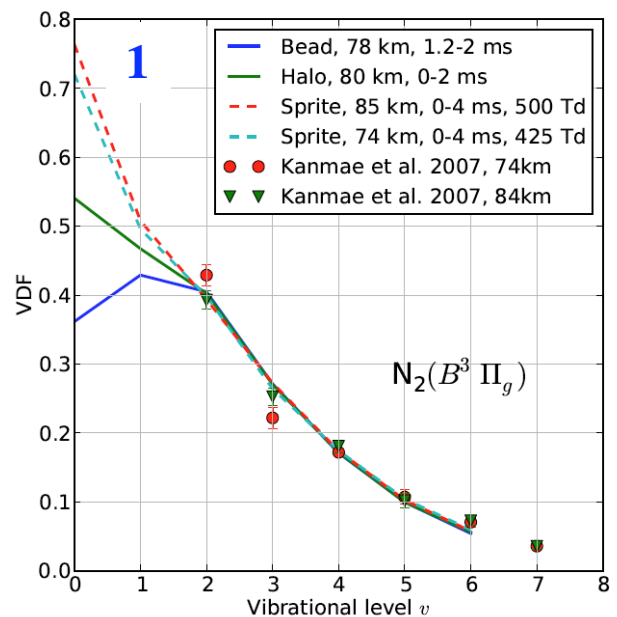


Fig. 1: Calculated VDF of $N_2(B^3\Pi_g)$ for Sprites, Halos and Beads and experimental $N_2(B^3\Pi_g)$ VDF for Sprites.

However, according to Figure 1, there is a difference (between the 1PG N_2 VDFs of sprites, halos and beads) in the $v = 1$ level and, especially, in the $v = 0$ level where the normalized sprite bead vibrational population is approximately half that of sprites and 60 % lower than that of halos. This change in the relative vibrational populations of $N_2(B^3\Pi_g)$ involved in the NIR ($v = 0, 1$; core sprite region) and visible ($v = 2, 3, \dots$; top sprite region) emitting sprite regions can be the underlying reason that explains the change in the central core-to-top brightness ratio in sprites [8]. The consequence of

this is that strong optical emissions involving $N_2(B^3\Pi_g; v = 0)$ such as those at ~ 1046 nm and ~ 1231 nm corresponding to the N_2 -1PG (0,0) and (0,1) bands will also produce significant differences among the NIR spectroscopic patterns of sprites, halos and sprite beads.

Figure 2 shows that the $N_2(C^3\Pi_u)$ VDFs in sprites, halos and sprite beads clearly differ for $v = 0, 2$. For $v = 0$ the halos and sprite bead populations are 20 % above that of sprites while for $v = 2$, sprite densities are 40 % - 50 % above that of halos and sprite beads.

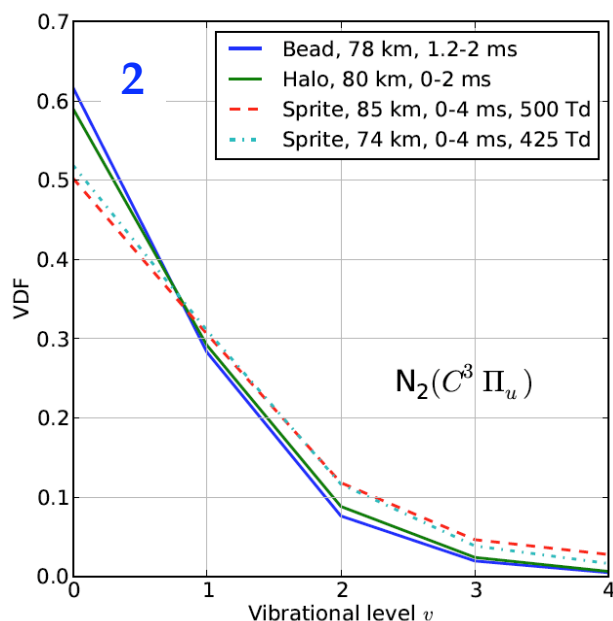


Fig. 2: Calculated VDF of $N_2(C^3\Pi_u)$ for Sprites, Halos and Beads.

For the less populated $v = 3, 4$ levels, the difference is less visible but still significant (sprite vibrational concentrations between 90 %, for $v = 3$, and 70 % for $v = 4$ above those of halos and sprite beads).

3. Conclusions

In this contribution we present calculations of the non-equilibrium VDFs of $N_2(B^3\Pi_g)$ 1PG and $N_2(C^3\Pi_u)$ 2PG corresponding to sprites, halos and sprite beads. The calculated VDFs have allowed us to generate synthetic spectra of sprites (74 km and 85 km), halos (80 km) and sprite beads (78 km) covering the NIR (up to 1800 nm), visible (450 nm - 750 nm) and near UV - violet (250 nm - 450 nm) spectral ranges. We have found that the calculated $N_2(B^3\Pi_g)$ VDFs of sprites, halos and sprite beads are significantly different for $v = 1$ and, especially, for $v = 0$, where NIR emissions are important. Besides this, our calculated VDFs of $N_2(B^3\Pi_g)$ agree quite well [9]-[10] with the measured sprite VDFs of the

N_2 -1PG visible spectrum (including the transitions $\Delta v = 1, 2, 3$) recorded by [6]. In consequence, our results indicate that, while visible spectra are quite the same, the calculated NIR spectra of sprites, halos and sprite beads exhibit significant differences that could be above sensitivity and, consequently, detectable, in the transitions (0,1) (888.3 nm), (0,0) (1046 nm) and (0,1) (1231 nm). Finally, our calculations also predict different spectral features in the $N_2(C^3\Pi_u)$ 2PG near UV emissions from sprites, halos and sprite beads corresponding to bands originating from higher vibrational numbers $v > 0$ that could be detected from balloons (35 km) and/or space platforms.

4. References

- [1] Gordillo-Vázquez, F. J., A. Luque, M. Simek, J. Geophys. Res. (Space Phys.) **116**, A09319, doi:10.1029/2011JA016652, 2011.
- [2] Gordillo-Vázquez, F. J., A. Luque, M. Simek, J. Geophys. Res. (Space Phys.) (submitted), 2012.
- [3] Simek, M., G. Dilecce, S. DeBenedictis, Plasma Chem. Plasma Proc., **15** (3), 310 427–449, 1995.
- [4] Simek, M., J. Phys. D: Appl. Phys., **35**, 1967, doi:10.1088/0022-3727/35/16/311, 2002.
- [5] Gilmore, F. R., R. R. Laher, P. J. Espy, J. Phys. Chem. Ref. Data, **21**, 1005, doi:10.1063/1.555910, 1992.
- [6] Kanmae, T., H. C. Stenbaek-Nielsen, M. G. McHarg, Geophys. Res. Lett., **34**, L07,810, doi:10.1029/2006GL028608, 2007.
- [7] Wescott, E. M., H. C. Stenbaek-Nielsen, D. D. Sentman, M. J. Heavner, D. R. Moudry, F. T. S. Sabbas, J. Geophys. Res. (Space Phys.), **106**, 10,467, doi: 10.1029/2000JA000182, 2001.
- [8] Sieftring, C. L., J. S. Morrill, D. D. Sentman, M. J. Heavner, J. Geophys. Res. (Space Phys.), **115**, A00E57, doi:10.1029/2009JA014862, 2010.
- [9] Gordillo-Vázquez, F. J., J. Geophys. Res. (Space Phys.), **115**, A00E25, doi:10.1029/2009JA014688, 2010.
- [10] Luque, A., and F. J. Gordillo-Vázquez, J. Geophys. Res. (Space Phys.), **116**, A02306, doi:10.1029/2010JA015952, 2011.